Pergamon

Int. J. Heat Mass Transfer. Vol. 40. No. 2. pp. 213–222, 1997

0017-9310/97 $15.00+0.00

PII: S0017-9310(96)00139-1

Evaluation of discrete ordinates method for radiative transfer in rectangular furnaces

NEVIN SELÇUK and NURAY KAYAKOL

Department of Chemical Engineering, Middle East Technical University, Ankara 06531, Turkey

(*Received* 25 *October* 1995 *and in final form* 10 *April* 1996)

Abstract—The discrete ordinates method (DOM) and discrete transfer method (DTM) were evaluated from the viewpoints of both predictive accuracy and computational economy by comparing their predictions with exact solutions available from a box-shaped enclosure problem with steep temperature gradients. Comparative testing shows that the S_4 approximation produces better accuracy in radiative energy source term than in flux density in three orders of magnitude less CPU time than that required by the DTM. The S_4 approximation can therefore be recommended to be used in conjunction with CFD codes. Copyright © 1996 Elsevier Science Ltd.

1. INTRODUCTION

The ever-increasing consumption of limited energy sources on one hand and environmental concern over the reduction of combustion-generated pollutant emission on the other, necessitates improvement of thermal and emission performances of combustion systems burning natural gas, oil and coal. This can be achieved by developing mathematical models which could eventually be used for the design of environmentally acceptable combustion systems with improved energy efficiency. Thermal radiation is the predominant mode of heat transfer at the high temperatures encountered in most industrial combustion chambers. Therefore, an adequate treatment of thermal radiation is essential to develop a mathematical model of combustion systems.

The exact (analytical or numerical) solution of integro-differential radiative transfer equation (RTE) is generally a formidable task. Although there have been a few attempts to formulate RTE for non-isothermal rectangular enclosures [1, 2], explicit solutions are only available for simplified situations such as black walls and constant properties etc. [3, 4]. Nevertheless exact solutions even for these simplest systems are needed, as they can serve as benchmarks against which the accuracy of approximate solutions is tested.

There is growing interest in approximate multidimensional radiative heat transfer models mainly in response to the need for accurate, flexible and computationally economic models which couple easily with the differential equations governing the transport of mass, momentum, species and energy in comprehensive models for turbulent, reacting and radiating flows.

The available approximate solution methods can be classified into four groups: Hottel's zone method, Monte-Carlo methods, flux-type methods and the DTM (discrete transfer method) which combines virtues of the first three. The Hottel's zone method and the Monte-Carlo technique have long been accepted as the most accurate methods for calculating radiative transfer. These traditional methods, however, have not found application in comprehensive combustion modeling due to their large computational time and storage capacity. At the same time, neither of these models requiring the solution of simultaneous algebraic equations are compatible with the solutions of the differential equations governing the transport of mass, momentum, species and energy in comprehensive numerical models.

The so-called flux methods which provide an alternative but less accurate method of solution convert the integro-differential equation into differential equations by discretization of angular variation of radiative intensity [5–7]. Being differential in form these equations are ideally suited to numerical solution simultaneously with the flow equations. Therefore, the flux methods offer a very high degree of computational economy and for this reason they have been widely employed in combustion models. All conventional flux methods suffer from the difficulty in application to complex geometries whereas some of them suffer from an inadequate number of directional fluxes and a lack of coupling between these fluxes. The DOM (discrete ordinates method), which conceptually is an extension of flux methods, corrects these defects. The DOM achieves a solution by solving the exact RTE for a set of discrete directions spanning the angle range of 4π. Apart from the obvious ease with which the method can be incorporated into computational fluid dynamics (CFD) calculations, it is relatively easy to code and requires single formulations to invoke higher order approximation. This method was first suggested by Chandrasekhar [8] for one-dimensional astrophysics problems. More recently, Carlson and

NOMENCLATURE

A, B, C	control volume face areas in x, y, z direction [m^2]
d	slope of the axial temperature curve
E	emissive power [W m^{-2}]
I	radiant intensity [W m^{-2} sr^{-1}]
k_a	gas absorption coefficient [m^{-1}]
L	half of the side lengths of the rectangular enclosure [m]
ℓ	direction cosines
q	radiative heat flux [W m^{-2}]
q_{net}	net radiative heat flux [W m^{-2}]
$\mathbf{r}$	position vector
S	radiative energy source term [W m^{-3}]
T	temperature [K]
v_p	volume of pth control volume [m^3]
w_m	weight function in a direction m
x, y, z	co-ordinate axes in Cartesian geometry
z'	dimensionless axial distance.

Greek symbols

α	finite-difference weighting factor
θ	polar angle
μ, η, ξ	direction cosines in x, y, z directions
σ	Stefan-Boltzmann constant
τ	optical thickness
ϕ	azimuthal angle
Ω	direction vector of radiant intensity.

Subscripts

burner	burner wall
bw	black wall
e	end-face
end	end wall
g	gas
i	inlet
m	discrete direction
max	maximum
o	reference value
p	control volume centre
r	reference-face
side	side wall
w	wall.

Superscripts

+	leaving
−	arriving
~	dimensionless.

Abbreviations

CFD	computational fluid dynamics
DOM	discrete ordinates method
DTM	discrete transfer method
DT64	discrete transfer using 64 ray per wall node
RTE	radiative transfer equation.

Lathrop [9] developed the DOM to solve multi-dimensional neutron transport problems. Over the past decade, the method has been applied to one- [10, 11] and multi-dimensional [12–21] radiative heat transfer problems.

Previously published multi-dimensional evaluations of the accuracy of the DOM have taken three forms:

(1) The DOM has been employed as part of a complete prediction procedure: (i) the predicted temperature distributions have been compared with experimentally determined data [12]. Discrepancies between predicted and measured values may be partly due to the errors in the experimentally determined data; even if the experimentally determined data are correct, it is impossible to decide whether discrepancies in the predicted temperature and radiative heat flux distributions are attributable to the radiation model employed, or to inaccuracies in the models used for the prediction of flow, reaction, etc. (ii) The predicted temperature and heat flux distributions have been compared with those predicted by the six-flux model [13]. However, assessment has been carried out on a small laboratory furnace where radiation was not the controlling heat transfer mechanism.

(2) The accuracy of DOM has been tested in isolation from the modeling of other physical processes. Testing has taken two forms: (i) the model has been employed by using prescribed radiative energy source term distributions (zero [14, 15] or uniform [14, 16, 17]) and comparing the predicted temperature and radiative heat flux distributions with the Hottel's zone method or exact solutions. This procedure for the evaluation of the accuracy of the DOM suffers from two major disadvantages: (a) even if acceptably accurate predictions are obtained for the uniform source term distributions, there is no certainty that similarly accurate predictions will be produced for the highly non-uniform distributions encountered in operating furnaces and combustors; (b) considering the iterative sequence of the solution in the complete prediction procedure, input data provided should be temperature distributions, and the predicted and tested quantities should be radiative heat flux and radiative energy source term distributions. (ii) The model has been tested by using prescribed temperature distributions (uniform [15, 16, 18] or non-uniform [16, 17, 19]) and comparing the predicted heat flux distributions with those predicted by the Hottel's zone method. This procedure has two drawbacks: (a) although uniform

temperature distributions are computationally convenient they do not even approximately represent the extremely non-uniform distributions encountered in operating furnaces and combustors; (b) the use of Hottel's zone method for testing the radiative heat flux distributions of an enclosure problem with steep temperature gradients requires finer zoning, which can be computationally inefficient due to extensive machine storage capacity and time.

(3) The DOM has been tested by calculating wall heat flux distribution from measured temperature distribution and comparing the predictions with measurements [13, 20]. This assessment procedure can be misleading due to the decoupling between the radiation model and the models used for the prediction of flow, reaction, etc.

What is required at the present time is testing of the accuracy and computational economy of the two radiation models (namely the DOM and the DTM) extensively used as part of complete prediction procedures in the past decade, in isolation from the models of flow and reaction, on problems with highly non-uniform gas temperature distribution typical of operating furnaces. Assessment of the predictive accuracy of the DTM has been reported in detail in an earlier paper [21].

In the present paper, the DOM is applied to solve the radiative heat transfer problems in two test cases for which analytical and numerical exact solutions are available. The first is a one-dimensional slab containing an absorbing–emitting medium with uniform gas temperature [22], the second is a box-shaped enclosure problem based on data reported previously on a large-scale experimental furnace with steep temperature gradients. The test cases are chosen to benchmark the DOM against exact solutions [3] and the other most widely used model, namely the DTM. The DOM and the DTM are also evaluated from the viewpoint of computational economy.

2. DESCRIPTION OF THE METHOD

The physical situation to be considered is that of an enclosure containing an absorbing–emitting, non-scattering radiatively gray medium whose absorption coefficient is the same at all points, and of known magnitude. Values of black-body emissive power are assumed to be available at all points within the enclosed medium and at all points on the interior bounding surfaces of the enclosure which are assumed to be black.

The discrete ordinates representation of RTE for an absorbing–emitting gray medium in a rectangular coordinate system (see Fig. 1) can be written as:

$$\mu_m \frac{\partial I^m}{\partial x} + \eta_m \frac{\partial I^m}{\partial y} + \xi_m \frac{\partial I^m}{\partial z} = -k_a I^m + k_a I_b \quad (1)$$

where I^m [$\equiv I(x, y, z; \mu_m, \eta_m, \xi_m)$] is the total radiation intensity at position (x, y, z) in the discrete direction

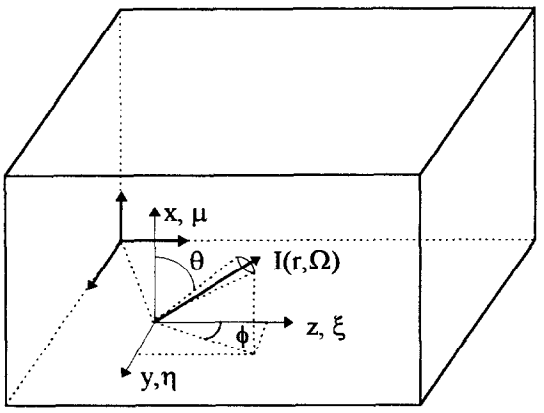

Fig. 1. Coordinate system.

Ω_m ($\mu_m = \cos\theta$, $\eta_m = \sin\theta\sin\phi$, $\xi_m = \sin\theta\cos\phi$), k_a absorption coefficient of medium, I_b the total black-body radiation intensity at the temperature of the medium. If the surface bounding the medium is assumed to be black, then the radiative boundary condition for equation (1) is given by

$$I^m = I_{bw} = \sigma T_w^4/\pi \quad (2)$$

where I_{bw} is the blackbody radiation intensity at the temperature of the surface, T_w. Equations (1) and (2) represent m coupled partial differential equations for the m intensities, I^m.

The finite-difference form of equation (1) can be obtained by multiplying equation (1) by $dx \cdot dy \cdot dz$ and integrating over the control volume as follows

$$\mu_m A(I^m_{xe} - I^m_{xr}) + \eta_m B(I^m_{ye} - I^m_{yr}) + \xi_m C(I^m_{ze} - I^m_{zr}) = -k_a v_p I^m_p + k_a v_p I_b \quad (3)$$

where I^m_p is cell-center intensity and $I^m_{xr}, I^m_{xe}, I^m_{yr}, I^m_{ye}, I^m_{zr}, I^m_{ze}$ are the intensities at each face of control volume. If the face intensities I^m_{xr}, I^m_{yr}, and I^m_{zr} are assumed to be known from boundary conditions for a control volume adjacent to a boundary of the enclosure, the following relationships [14] can be used to eliminate the unknown face intensities I^m_{xe}, I^m_{ye} and I^m_{ze} in equation (3).

$$I^m_p = \alpha I^m_{xe} + (1-\alpha) I^m_{xr} \quad (4)$$

$$I^m_p = \alpha I^m_{ye} + (1-\alpha) I^m_{yr} \quad (5)$$

$$I^m_p = \alpha I^m_{ze} + (1-\alpha) I^m_{zr}. \quad (6)$$

The finite-difference weighting factor $\alpha = 0.5$ represents the second-order diamond difference scheme proposed by Carlson and Lathrop [9]. After some rearrangement the cell-center intensity, I^m_p may be evaluated as

$$I_p^m = \frac{\mu_m A I_{xr}^m + \eta_m B I_{yr}^m + \xi_m C I_{zr}^m + \alpha k_a v_p I_b}{\mu_m A + \eta_m B + \xi_m C + \alpha k_a v_p} \quad (7)$$

where

$$A = \Delta y \Delta z, \quad B = \Delta x \Delta z, \quad C = \Delta x \Delta y. \quad (8)$$

Every I^m value on every cell-center and faces of control volume can be computed by stepping from control volume to control volume. The direction of recursive evaluation is in accord with the direction of physical propagation of radiation beam as defined by (μ_m, η_m, ξ_m).

Once the intensity distribution is determined, quantities of interest such as radiative flux and energy source term distributions can be readily evaluated. The net radiation heat flux on a wall is calculated as

$$q_{net} = q^+ - q^- \quad (9)$$

where q^+ and q^- are leaving and arriving wall heat fluxes, respectively. For the physical situation under consideration, q^+ and q^- can be written as

$$q^+ = \pi I_{bw} = \sigma T_w^4 \quad (10)$$

$$q^- = \int_{2\pi} \ell I \mathrm{d}\Omega = \sum_m w_m \ell I^m. \quad (11)$$

The radiative energy source term distribution for problems where prescribed temperature distributions are available is expressed as

$$S = k_a\left(4\pi I_b - \int_{4\pi} I \mathrm{d}\Omega\right) = k_a(4\pi I_b - \sum_m w_m I_p^m). \quad (12)$$

As can be seen from equations (11) and (12), quadrature schemes are required for approximating the integrals. Therefore the accuracy of discrete ordinates solutions depends on the choice of the angular quadrature scheme. Schemes for one-dimensional radiative transfer problems are well developed but their accuracies are significantly dependent on the physical nature of the problem. However, the extension of these angular quadrature schemes to multi-dimensional radiative transfer problems is not always obvious and straightforward. The choice of scheme is arbitrary although restrictions on the directions and weights arise from the need to preserve symmetries and invariance properties of the physical system [9].

3. PERFORMANCE OF DISCRETE ORDINATES METHOD

The DOM has been evaluated on two test cases for which analytical and numerical exact solutions are available. The first being a one-dimensional slab containing an absorbing–emitting medium with uniform gas temperature [22], the second being a box-shaped enclosure problem based on data reported previously on a large-scale experimental furnace with steep temperature gradients [3].

3.1. *A one-dimensional slab containing an absorbing–emitting medium with uniform gas temperature*

The physical situation is two infinitely large parallel cold black plates containing an absorbing–emitting medium with uniform temperature. Wall heat fluxes calculated by using DOM for varying optical thicknesses between 0.1 and 3.0 and for different angular quadrature schemes,were compared with the exact analytical solutions [22].

Figure 2 shows the comparison between exact solutions and DOM predictions using two different angular quadrature schemes; S_n (S_2 and S_4 [15]) and $S_{n'}$ ($S_{2'}$ and $S_{4'}$ [15]). As shown in Fig. 2, different angular

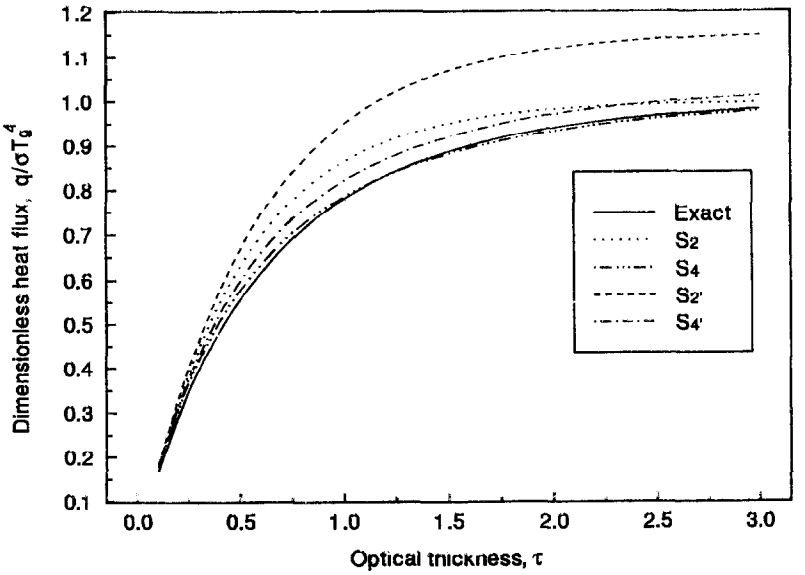

Fig. 2. Comparison between exact solutions and DOM predictions of dimensionless heat fluxes.

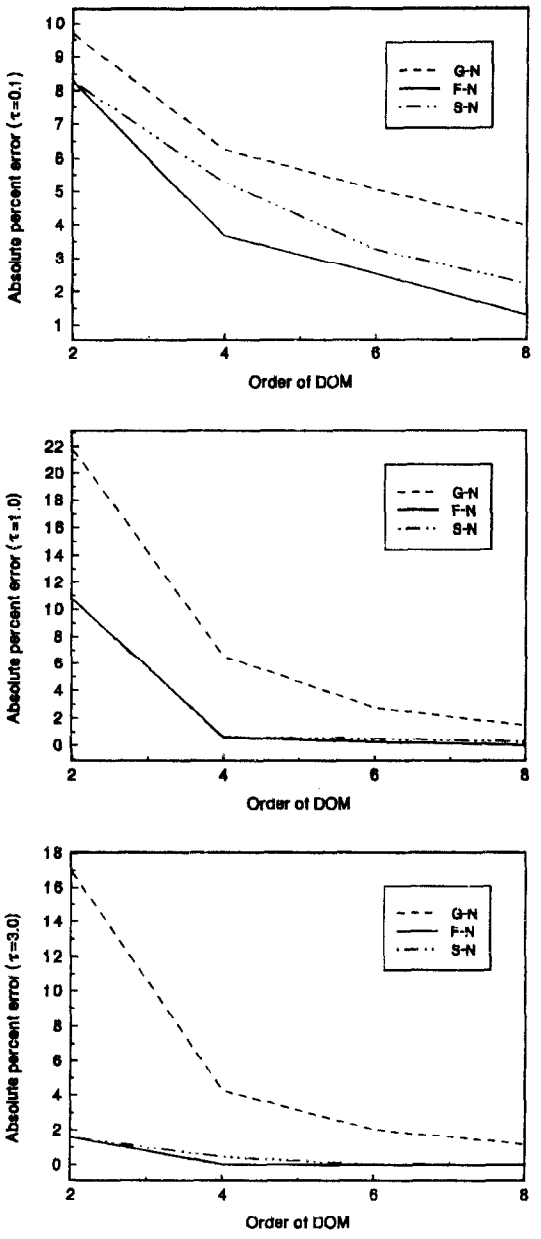

Fig. 3. Variation of solution errors with the order for S-N, G-N and F-N angular quadrature schemes.

quadrature schemes (i.e. the selection of discrete directions and associated weights) may result in considerably different accuracies. S_2 significantly deviates from the exact solution. S_n produces better agreement than $S_{n'}$ due to the failure of $S_{n'}$ to satisfy the half range flux conditions [15].

Figure 3 illustrates variation of absolute percentage errors in wall heat fluxes with the order of DOM using S_n (S-N), Gaussian (G-N) and Fiveland (F-N) [10] angular quadrature schemes for various optical thicknesses. As can be seen from Fig. 3, for all optical thicknesses, percentage errors in wall heat fluxes decrease with the order of DOM, irrespective of the angular quadrature schemes. It can also be noted that low orders of G-N do not predict the half range heat fluxes accurately as they do not correctly integrate the half range first-order moment of intensity. To achieve reasonable accuracy, higher order approximations of G-N are necessary at the expense of computational inefficiency unless S-N or F-N schemes are employed. Wall heat fluxes predicted by both S-N and F-N compare well with the exact solution as they both satisfy the first-moment for half range. It can be concluded that for the test problem under consideration the half range integrals in the boundary conditions are more important to solution accuracy than the full range integrals in the RTE.

Figure 4 indicates the variation of absolute percentage errors in wall heat fluxes predicted by the DTM with number of rays for various optical thicknesses. As can be seen from Fig. 4, the accuracy increases with increasing ray numbers and only slight improvement is obtained after a certain number of rays.

3.2. *A three-dimensional rectangular enclosure problem containing an absorbing–emitting medium with steep temperature gradients*

The accuracy of DOM for three-dimensional radiative heat transfer has been assessed by applying this radiation model to the prediction of distributions of radiative flux density and radiative energy source term of a highly demanding rectangular enclosure problem with a steep temperature gradient and a non-scattering medium of small optical thickness and by comparing its predictions with exact solutions produced previously [3]. The rectangular enclosure under consideration has interior black walls and an absorbing–emitting medium of constant properties. The problem was based on data taken from a large-scale experimental furnace with steep temperature gradients typical of operating furnaces.

The experimental furnace under consideration is horizontal, of tunnel type with a square cross-section, it is fired horizontally from the center of the left end wall, which is the burner wall, with a mixture of oil and gas with no swirl, and operates at atmospheric pressure, the four side walls are water cooled, and the burner and back end walls are refractory. Table 1 shows the complete dimensionless data obtained from the experimental furnace and used as input data for both the exact solution and DOM. A detailed description of data can be found elsewhere [3].

The numerical solution procedure in the present work has been based on the method of Carlson and Lathrop [9]. RTE has been reduced to conservative finite difference form using the control volume method and the diamond difference scheme with set-to-zero negative intensity fix-up. Quadrature points and weights are calculated by the moment-matching technique proposed by Carlson and Lathrop [9]. The quadrature scheme satisfies the zeroth and second moments for full range (i.e. 4π); and the first moment for half range (i.e. 2π). The S_n discrete ordinate for-

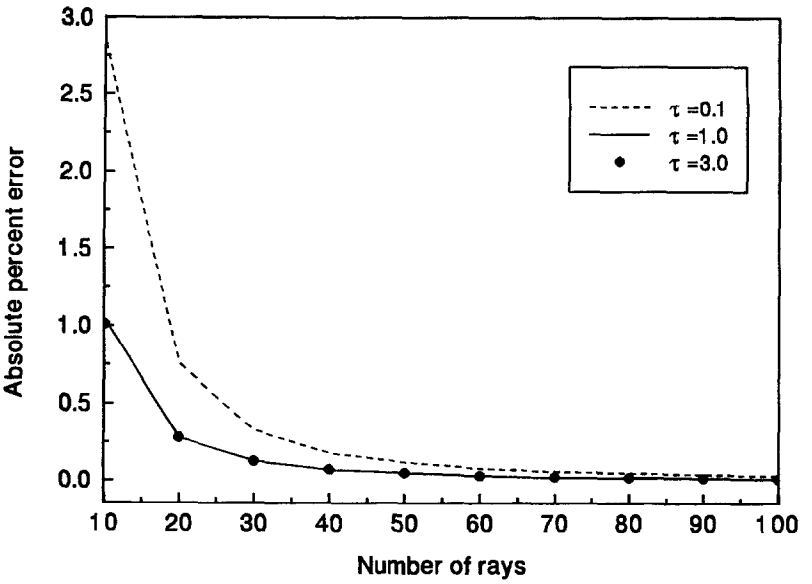

Fig. 4. Variation of solution errors with number of rays for DTM.

Table 1. Dimensionless data fed to the exact solution and S_n method program

Dimensions of the furnace	$\tilde{L}_x = 1,\ \tilde{L}_y = 1,\ \tilde{L}_z = 6$
Optical thickness	$\tau_0 = 1/6$
Wall black-body intensities	$(\tilde{I}_{bw})_{side} = 0.0020$ $(\tilde{I}_{bw})_{burner} = 0.0574$ $(\tilde{I}_{bw})_{end} = 0.0167$
Gas temperatures	$\tilde{T}_i = 0.1775$ $\tilde{T}_e = 0.6222$ $\tilde{T}_{max} = 1$
Position of the peak	$z'_{max} = 0.8$
Slope of gas temperature distribution at furnace exit	$d_e = -0.220$

Reference values used to make the experimental data dimensionless: $L_0 = 0.48$ m, $T_0 = 1673$K, $E_0 = 4.4419 \times 10^5$ W m^{-2}, $I_0 = 1.4139 \times 10^5$ W m^{-2} sr^{-1}.

mulation requires $n(n+2)$ discrete directions for $n = 2, 4, 6, \ldots$ The number of directions required in a completely symmetric arrangement is found to be $n(n+2)/8$, i.e. the total number of directions per octant. The quadrature ordinates and weights for the S_4 approximation are listed in Table 2. The test enclosure has been subdivided into $4 \times 4 \times 24$ control volumes in x, y, z directions, respectively. In an earlier paper [21], the DTM had been applied to the predictions of the radiative flux density and energy source term of the same enclosure problem. Comparisons of the DTM predictions employing different ray numbers and control volumes with the exact solutions indicated that the DTM provides radiative flux density and energy source term distributions in close agreement with the exact solutions for 64 rays and for the same subdivision of the enclosure. For comparative testing of the two methods from the viewpoint of both the accuracy and computational economy the predictions of both will be presented here.

3.2.1. *Flux density distributions.* Figure 5 illustrates the comparison between the point values of the dimensionless heat flux density to the side wall in the positive x-direction predicted by the S_4 approximations, the DT64 and exact solutions for surface grid points. Points on the lines $(\tilde{x} = 1, \tilde{y} = 0.25, \tilde{z})$ and $(\tilde{x} = 1, \tilde{y} = 0.75, \tilde{z})$ represent points near the center of the face and near the corner of the face, respectively. As can be seen from Fig. 5, the flux densities to the side wall predicted by the S_4 are found to be in good agreement with the exact solutions over the whole length of the enclosure. A condensed comparison of the S_4 and the DT64 predictions of flux densities is contained in Table 3. As can be seen from Table 3, both methods produce acceptable accuracies although the average absolute error produced by the S_4 is two times higher than that produced by the DT64.

Table 2. S_4 angular quadrature scheme the first octant

Direction number	Ordinates μ_m	η_m	ξ_m	Weight w_m
1	0.9082483	0.2958759	0.2958759	0.5235987
2	0.2958759	0.9082483	0.2958759	0.5235987
3	0.2958759	0.2958759	0.9082483	0.5235987

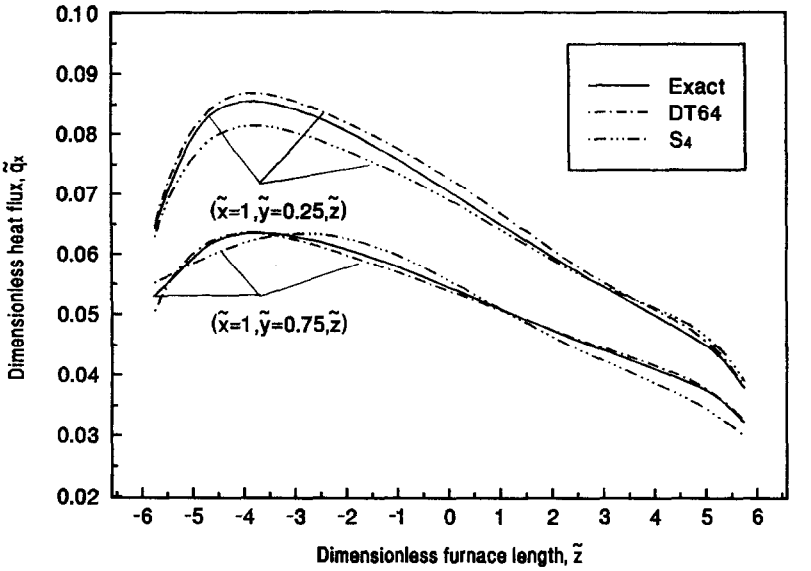

Fig. 5. Comparison between the exact values and the DTM and the S_4 predictions of dimensionless flux densities to the side wall.

Table 3. Comparison of the S_4 and the DT64 predictions of dimensionless flux densities for surface grid points

Method	Average absolute error ($\tilde{x}=1,\tilde{y}=0.75,\tilde{z}$)	($\tilde{x}=1,\tilde{y}=0.25,\tilde{z}$)	Side wall	Maximum percentage error
DT64	1.12	1.93	1.52	10.21
S_4	3.40	2.87	3.13	9.43

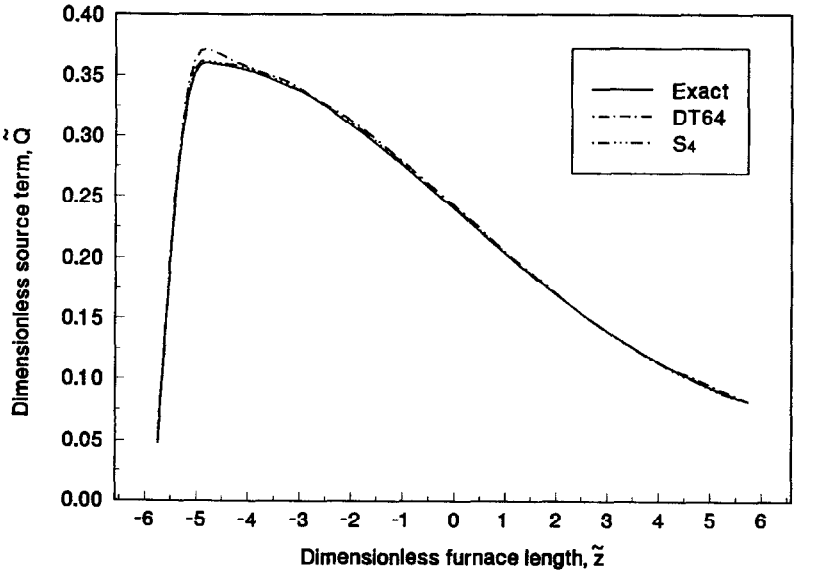

Fig. 6. Comparison between the exact values and the DTM and the S_4 predictions of dimensionless radiative energy source terms along ($\tilde{x}=0.25,\tilde{y}=0.25,\tilde{z}$).

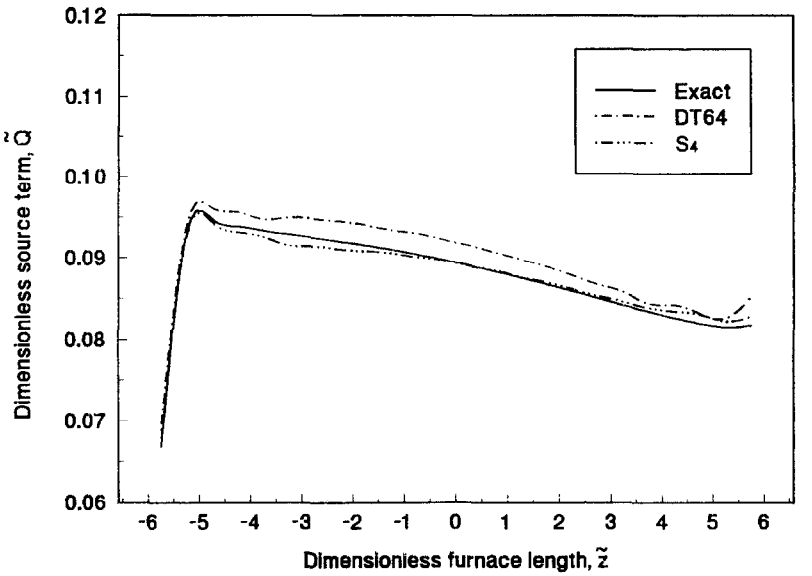

Fig. 7. Comparison between the exact values and the DTM and the S_4 predictions of dimensionless radiative energy source terms along ($\tilde{x} = 0.75, \tilde{y} = 0.25, \tilde{z}$).

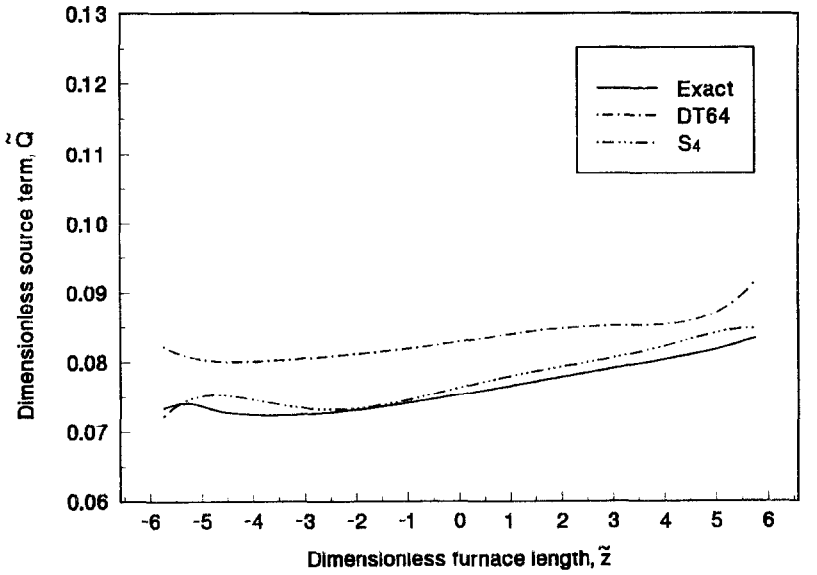

Fig. 8. Comparison between the exact values and the DTM and the S_4 predictions of dimensionless radiative energy source terms along ($\tilde{x} = 0.75, \tilde{y} = 0.75, \tilde{z}$).

Table 4. Comparison of the S_4 and the DT64 predictions of dimensionless source term distributions for medium grid points

Method	Average absolute error ($\tilde{x} = 0.75, \tilde{y} = 0.75, \tilde{z}$)	($\tilde{x} = 0.75, \tilde{y} = 0.25, \tilde{z}$)	($\tilde{x} = 0.25, \tilde{y} = 0.25, \tilde{z}$)	Maximum percentage error
DT64	9.36	2.27	1.35	11.64
S_4	1.75	0.62	0.63	3.66

Table 5. Comparisons of the S_4 and the DT64 predictions of the percentage errors in generated and removed radiative energy

Method	Percentage error in generation	Percentage error in removal
DT64	−2.34	−2.12
S_4	0.29	0.29

3.2.2. *Source term distributions.* Figure 6 shows the comparison between the S_4 and the DT64 predictions of dimensionless source term distributions and exact values for points $(\bar{x} = 0.25, \bar{y} = 0.25, \bar{z})$. These grid points represent the points at the center of the row of control volumes nearest to the furnace axis. It can be seen that the trend of the distributions predicted by the S_4 and the DT64 is the same as that of the exact distributions which follow the physically expected trend, rising steeply from the burner wall onward, going through a maximum and decreasing continuously toward the exit. The maximum of the source term distribution occurs at the same location as the maximum of temperature distribution.

Figures 7 and 8 illustrate the comparison between the exact values of dimensionless source term and distributions predicted by the S_4 and the DT64 for grid points $(\bar{x} = 0.75, \bar{y} = 0.25, \bar{z})$ and $(\bar{x} = 0.75, \bar{y} = 0.75, \bar{z})$. These grid points represent the medium points nearer to the side wall and near the corner of the enclosure, respectively. A condensed comparison of the S_4 and the DT64 predictions of source term distributions is contained in Table 4. As can be seen from Table 4, the maximum point percentage error produced by the S_4 is approximately one-third of that produced by the DT64. It can be noted that the S_4 produces smaller average absolute errors than the DT64. The CPU times for the S_4 and the DT64 using the IBM Risc/6000 Model 590 are 1308 and 2.3 s, respectively. It can therefore be concluded that the S_4 approximation is not only more accurate but also computationally more efficient than the DT64.

To provide a global check on the accuracy of the S_4 predictions, the total rate of removal of radiative energy through walls and the total rate of generation of radiative energy within the enclosed medium have been evaluated and compared with the exact values [3]. Table 5 shows the errors in generated and removed radiative energy produced by the S_4 and the DT64 predictions. As can be seen from Table 5, the percentage errors in generated and removed radiative energy are equal for the S_4 predictions, but almost equal for the DT64. The discrepancy encountered in the DT64 can be considered to be due to the evaluation of radiative energy source term through the method originally suggested by Shah [22].

4. CONCLUSIONS

The S_4 discrete ordinates approximation and discrete transfer methods have been applied to the predictions of the distributions of radiative flux density and energy source term of a black-walled rectangular enclosure problem. The problem was based on data taken from a large-scale experimental furnace with steep temperature gradients typical of operating furnaces. The accuracy of the models have been tested by comparing their predictions with the exact solutions reported earlier in the literature. Comparisons show that the S_4 approximation produces better accuracy in radiative energy source term than in flux density to the side wall. Comparative testing of the S_4 approximation and discrete transfer methods indicate that their predictions are in good agreement with the exact solutions and that the S_4 approximation requires a CPU time three orders of magnitude less than that required by discrete transfer method. Therefore, the S_4 approximation is a better alternative to be used as part of a complete prediction procedure.

REFERENCES

1. P. Cheng, Exact solutions and differential approximation for multi-dimensional radiative transfer in Cartesian coordinate configuration, *Prog. Astronaut. Aeronaut.* **31**, 269–308 (1972).
2. A. L. Crosbie and L. C. Lee, Relation between multidimensional radiative transfer in cylindrical and rectangular coordinates with anisotropic scattering, *J. Quant. Spectrosc. Radiat. Transfer* **38**, 231–241 (1987).
3. N. Selçuk, Exact solutions for radiative heat transfer in box-shaped furnaces, *J. Heat Transfer* **107**, 648–655 (1985).
4. N. Selçuk and Z. Tahiroglu, Exact numerical solutions for radiative heat transfer in cylindrical furnaces, *Int. J. Numer. Meth. Engng* **26**, 1201–1212 (1988).
5. N. Selçuk, Evaluation of flux models for radiative transfer in rectangular furnaces, *Int. J. Heat Mass Transfer* **31**, 1477–1482 (1988).
6. N. Selçuk, Evaluation of flux models for radiative transfer in cylindrical furnaces, *Int. J. Heat Mass Transfer* **32**, 620–624 (1989).
7. N. Selçuk, Evaluation of spherical harmonics approximation for radiative transfer in cylindrical furnaces, *Int. J. Heat Mass Transfer* **33**, 579–581 (1990).
8. S. Chandrasekhar, *Radiative Transfer*. Dover, New York (1960).
9. B. G. Carlson and K. D. Lathrop, Transport theory—the method of discrete ordinates, in *Computing Methods in Reactor Physics* (Edited by H. Greenspan, C. N. Kelber and D. Orkent), pp. 165–266. Gordon & Breach, New York (1968).
10. W. A. Fiveland, Discrete ordinate methods for radiative heat transfer in isotropically and anisotropically scattering media, *J. Heat Transfer* **109**, 809–812 (1987).
11. J. S. Truelove, An evaluation of the discrete ordinates approximation for radiative transfer in an absorbing, emitting, and scattering planar medium. HTFS Report no. R8478 (1976).
12. E. E. Khalil and J. S. Truelove, Calculation of heat transfer in a large gas fired furnace. HTFS Report no. R8747 (1977).
13. A. S. Jamaluddin and P. J. Smith, Predicting radiative transfer in axisymmetric cylindrical enclosures using discrete ordinates method, *Combust. Sci. Technol.* **62**, 173–186 (1988).
14. W. A. Fiveland, Three-dimensional radiative heat transfer solutions by discrete ordinates method, *J. Thermophys.* **2**, 309–316 (1988).

15. J. S. Truelove, Discrete ordinates solutions of radiation transport equation, *J. Heat Transfer* **109,** 1048–1051 (1987).
16. A. S. Jamaluddin and P. J. Smith, Predicting radiative transfer in rectangular enclosures using discrete ordinates method, *Combust. Sci. Technol.* **59,** 321–340 (1988).
17. D. J. Hyde and J. S. Truelove, The discrete ordinate approximation for multi-dimensional radiant heat transfer in furnaces. HTFS Report no. R8502 (1977).
18. W. A. Fiveland, Discrete ordinates solutions of transport equations for rectangular enclosures, *J. Heat Transfer* **106,** 699–706 (1984).
19. A. S. Jamaluddin and P. J. Smith, Discrete-ordinates solutions of radiative transfer in nonaxisymmetric cylindrical enclosures, *J. Thermophys.* **6,** 242–245 (1992).
20. W. A. Fiveland, A discrete ordinates method for predicting radiative transfer in axisymmetric enclosures, ASME paper 83-HT-20 (1982).
21. N. Selçuk and N. Kayakol, Evaluation of discrete transfer model for radiative transfer in combustors, *Proceedings of International Symp. on Radiative Heat Transfer*, ICHMT, Kuşadasi, Turkey (1995).
22. N. G. Shah, New method of computation of radiant heat transfer in combustion chambers. Ph.D. Thesis, University of London, London (1979).